Velocity-selected production of 2³S metastable positronium

C. Amsler,[1] M. Antonello,[2,3] A. Belov,[4] G. Bonomi,[5,6] R. S. Brusa,[7,8] M. Caccia,[2,3] A. Camper,[9] R. Caravita,[9,*] F. Castelli,[2,10] G. Cerchiari,[11] D. Comparat,[12] G. Consolati,[13,2] A. Demetrio,[14] L. Di Noto,[15,16] M. Doser,[9] M. Fanì,[15,16,9] S. Gerber,[9] A. Gligorova,[1] F. Guatieri,[7,8] P. Hackstock,[1] S. Haider,[9] A. Hinterberger,[9] H. Holmestad,[17] A. Kellerbauer,[11] O. Khalidova,[9] D. Krasnický,[16] V. Lagomarsino,[15,16] P. Lansonneur,[18] P. Lebrun,[18] C. Malbrunot,[9,1] S. Mariazzi,[7,8,†] V. Matveev,[4,19] S. R. Müller,[14] G. Nebbia,[20] P. Nedelec,[18] M. Oberthaler,[14] D. Pagano,[5,6] L. Penasa,[7,8] V. Petracek,[21] F. Prelz,[2] M. Prevedelli,[22] B. Rienaecker,[9] J. Robert,[12] O. M. Røhne,[17] A. Rotondi,[6,23] H. Sandaker,[17] R. Santoro,[2,3] L. Smestad,[9,24] F. Sorrentino,[15,16] G. Testera,[16] I. C. Tietje,[9] E. Widmann,[1] P. Yzombard,[11] C. Zimmer,[9,11,25] and N. Zurlo[6,26]

(The AEgIS Collaboration)

[1]*Stefan Meyer Institute for Subatomic Physics, Austrian Academy of Sciences, Boltzmanngasse 3, 1090 Vienna, Austria*
[2]*INFN, Sezione di Milano, Via Celoria 16, 20133 Milano, Italy*
[3]*Department of Science and High Technology, University of Insubria, Via Valleggio 11, 22100 Como, Italy*
[4]*Institute for Nuclear Research of the Russian Academy of Science, Moscow 117312, Russia*
[5]*Department of Mechanical and Industrial Engineering, University of Brescia, Via Branze 38, 25123 Brescia, Italy*
[6]*INFN Pavia, Via Bassi 6, 27100 Pavia, Italy*
[7]*Department of Physics, University of Trento, Via Sommarive 14, 38123 Povo, Trento, Italy*
[8]*TIFPA/INFN Trento, Via Sommarive 14, 38123 Povo, Trento, Italy*
[9]*Physics Department, CERN, 1211 Geneva 23, Switzerland*
[10]*Department of Physics "Aldo Pontremoli", Università degli Studi di Milano, Via Celoria 16, 20133 Milano, Italy*
[11]*Max Planck Institute for Nuclear Physics, Saupfercheckweg 1, 69117 Heidelberg, Germany*
[12]*Laboratoire Aimé Cotton, Université Paris-Sud, ENS Paris Saclay, CNRS, Université Paris-Saclay, 91405 Orsay Cedex, France*
[13]*Department of Aerospace Science and Technology, Politecnico di Milano, Via La Masa 34, 20156 Milano, Italy*
[14]*Kirchhoff-Institute for Physics, Heidelberg University, Im Neuenheimer Feld 227, 69120 Heidelberg, Germany*
[15]*Department of Physics, University of Genova, Via Dodecaneso 33, 16146 Genova, Italy*
[16]*INFN Genova, Via Dodecaneso 33, 16146 Genova, Italy*
[17]*Department of Physics, University of Oslo, Sem Saelandsvei 24, 0371 Oslo, Norway*
[18]*Institute of Nuclear Physics, CNRS/IN2p3, University of Lyon 1, 69622 Villeurbanne, France*
[19]*Joint Institute for Nuclear Research, Dubna 141980, Russia*
[20]*INFN Padova, Via Marzolo 8, 35131 Padova, Italy*
[21]*Czech Technical University, Prague, Brehová 7, 11519 Prague 1, Czech Republic*
[22]*University of Bologna, Viale Berti Pichat 6/2, 40126 Bologna, Italy*
[23]*Department of Physics, University of Pavia, Via Bassi 6, 27100 Pavia, Italy*
[24]*The Research Council of Norway, P.O. Box 564, 1327 Lysaker, Norway*
[25]*Department of Physics, Heidelberg University, Im Neuenheimer Feld 226, 69120 Heidelberg, Germany*
[26]*Department of Civil, Environmental, Architectural Engineering and Mathematics, University of Brescia, Via Branze 43, 25123 Brescia, Italy*

Positronium in the 2³S metastable state exhibits a low electrical polarizability and a long lifetime (1140 ns), making it a promising candidate for interferometry experiments with a neutral matter-antimatter system. In the present work, 2³S positronium is produced, in the absence of an electric field, via spontaneous radiative decay from the 3³P level populated with a 205-nm UV laser pulse. Thanks to the short temporal length of the pulse, 1.5 ns full width at half maximum, different velocity populations of a positronium cloud emitted from a nanochanneled positron-positronium converter were selected by delaying the excitation pulse with respect to the production instant. 2³S positronium atoms with velocity tuned between $7 \times 10^4 \, \mathrm{ms^{-1}}$ and $10 \times 10^4 \, \mathrm{ms^{-1}}$ were thus produced. Depending on the selected velocity, a 2³S production efficiency ranging from ∼0.8% to ∼1.7%, with respect to the total amount of emitted positronium, was obtained. The observed results give a branching ratio for the 3³P-2³S spontaneous decay of $(9.7 \pm 2.7)\%$. The present velocity selection technique could allow

---

*ruggero.caravita@cern.ch
†mariazzi@science.unitn.it

one to produce an almost monochromatic beam of $\sim 1 \times 10^3$ $2\,^3$S atoms with a velocity spread of $< 10^4 \, \mathrm{ms}^{-1}$ and an angular divergence of ~ 50 mrad.

I. INTRODUCTION

Positronium (Ps) is one of the few matter-antimatter systems (with antihydrogen and muonium) being considered for probing experimentally the gravitational interaction [1–5]. Several experimental schemes based on long-lived Ps beams have been proposed, either letting the atoms free-fall in a drift tube [6,7] or using a matter-wave atom interferometer [8] to measure their vertical displacement with a position-sensitive detector. Gravity (or any other force acting on the atoms) can then be worked out if the average velocity of the atoms is known [3,8].

All the suggested schemes involve laser excitation to long-lived excited states to overcome the lifetime limitation of the $1\,^3$S ground state (142 ns) where Ps is normally produced. An effective and widely adopted choice consists of laser exciting the atoms to the Rydberg levels, where lifetimes spanning from tens of microseconds up to several milliseconds can be obtained [9,10]. Atoms in Rydberg states are, in general, sensitive to electric-field gradients [11] which can modify their trajectories. This is due to their large electrical polarizability (up to $\sim 10^{-32} \, \mathrm{C\,m^2\,V^{-1}}$ for Ps in $n = 15$) [12,13]. Ps Rydberg sublevels with large electrical dipoles can be guided and focused [12,13] while the selective excitation to sublevels with low dipole moments has been proposed [14] as a method to minimize the deflection of Rydberg Ps in interferometric measurements with physical gratings [15].

An alternative way to produce a beam of long-lived Ps with lower electrical polarizability ($\sim 10^{-38} \, \mathrm{C\,m^2\,V^{-1}}$) consists of laser exciting the atoms to their $2\,^3$S metastable level [15], whose lifetime is 1.14 μs in vacuum and in the absence of an electric field [16]. A beam of $2\,^3$S Ps atoms (of known average velocity) has been shown to be suitable for improving the inertial sensitivity in proposed matter-wave interferometric layouts [8]. Moreover, the availability of $2\,^3$S Ps with an average velocity of $< 10^5 \, \mathrm{ms}^{-1}$ would allow keeping the interferometer compact in length ($L \lesssim 1$ m), thus easing the control of thermal and vibrational noise [17].

Producing fast $2\,^3$S Ps with energies of several electron volts has already been demonstrated via e^+ collisions with solid [18–20] or gaseous targets [21,22]. $2\,^3$S Ps atoms with a beam Maxwellian distribution at around 600 K (average speed of $> 1.4 \times 10^5 \, \mathrm{ms}^{-1}$) were also produced via Doppler-free two-photon excitation of ground-state atoms of Ps desorbed from metallic surfaces [23–25] and $1\,^3$S-$2\,^3$S two-photon excitation of Ps emitted from porous silicon [26]. Production of $2\,^3$S Ps via single-photon excitation of ground-state atoms to mixed $2\,^3$S-$2\,^3$P in electric fields [15] and the single-photon excitation of ground-state atoms to $3\,^3$P levels with subsequent radiative decay to $2\,^3$S [16] have been recently demonstrated. The reduction of the $2\,^3$S lifetime in electric fields due to Stark mixing has also been studied [16].

In the present work we investigate the feasibility of a source of metastable $2\,^3$S Ps with defined and tunable velocity

in the absence of an electric field. The $2\,^3$S level is populated by spontaneous radiative decay of laser-excited $3\,^3$P Ps atoms. The tuning of the $2\,^3$S Ps velocity is achieved by varying the delay of the $1\,^3$S-$3\,^3$P excitation pulse between 20 and 65 ns from the e^+ implantation time in a nanochanneled silicon e^+-Ps converter [27], thus selecting Ps populations emitted after different permanence times in the target [28,29] and consequently with different velocities [30,31].

II. EXPERIMENTAL METHODS

In our experiment, Ps is formed when ~ 7-ns bursts of $\sim 10^7$ e^+, prepared in the AEḡIS e^+ system (see Refs. [16,32,33] for a detailed description of the apparatus), are electromagnetically transported and implanted at 3.3 keV into a Si (111) p-type crystal where nanochannels were previously produced via electrochemical etching and thermal oxidized in air [16,33]. Ps produced inside the converter out-diffuses into vacuum through the nanochannels losing a fraction of its emission energy by collision with the walls. The Si target was kept at room temperature and e^+ were implanted into it with a spot of ~ 3 mm in size. Measurements previously performed on identical e^+-Ps converters indicated a wide angular emission of Ps from the nanochannels [16,33]. A schematic of the experimental chamber is illustrated in Fig. 1.

In the target region, e^+ are guided by a 25-mT magnetic field and focused by an electrostatic lens formed by the last
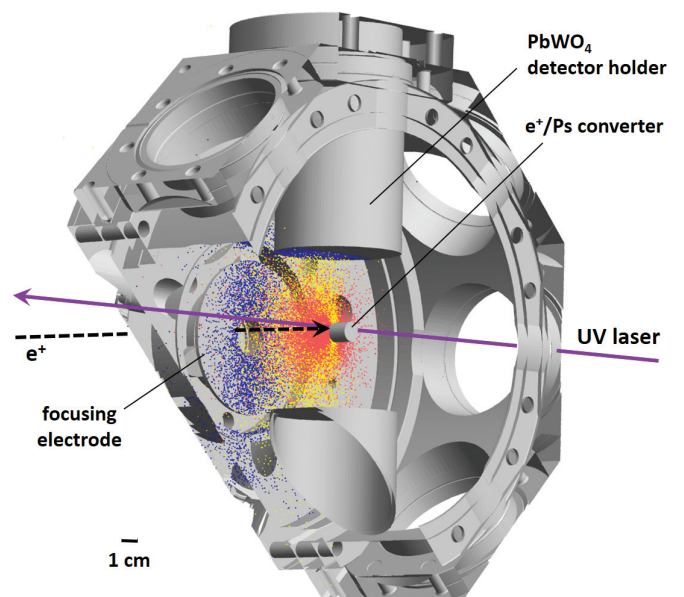

FIG. 1. Schematic of the experimental chamber with example Monte Carlo in-flight and collision annihilation distributions for a $1\,^3$S Ps population (light and dark red dots) and for a $2\,^3$S Ps population (yellow and blue dots). The line-shaped annihilation distribution of $2\,^3$S atoms is due to the UV-laser Doppler selection.

electrode of the transfer line set at -3000 V and the target kept at ground potential (see Fig. 1 for the geometry), inducing an electric field of about 300 V cm^{-1} in front of the converter. Since this electric field shortens considerably the 2^{3}S lifetime [13,16], for the present measurements the focusing electrode was switched off $\sim$5 ns after the e^+ implantation using a fast switch with a rise time of $\sim$15 ns (from -3000 to 0 V).

Ps emitted into vacuum was subsequently excited from the 1^{3}S ground state to the 3^{3}P sublevel manifold with an UV laser pulse set at a transition resonance wavelength of $\lambda_{UV} = (205.045 \pm 0.005)$ nm. The laser setup is described in detail elsewhere [33–35]. The UV pulse energy was kept above 60 μJ and the effective size of the spot about 3.0–3.5 mm full width at half maximum (FWHM) in both horizontal and vertical directions in front of the target. The laser beam was aligned grazing the target, and its position and size were monitored with a CCD camera on a 1-in. MACOR screen placed inside the vacuum region (a few centimeters away from the target). The UV pulse had a horizontal polarization (i.e., perpendicular to the target), a nearly Gaussian temporal profile with a FWHM of 1.5 ns, and a Gaussian-like spectral profile with a bandwidth of $\sigma_{UV} = 2\pi \times 120$ GHz.

The laser bandwidth is narrower than the Doppler profile of Ps emitted from the used e^+-Ps converter ($\sim$2$\pi \times$ 470 GHz, see Ref. [33]). As a consequence, the UV pulse selectively excites to 3^{3}P only the fraction of the emitted atoms with a velocity component parallel to the laser propagation axis, $v_\parallel$, with $|v_\parallel| < 2.5 \times 10^4$ ms^{-1}. Following the excitation, a fraction of Ps in the 3^{3}P sublevel spontaneously decays to 2^{3}S, emitting a 1312-nm photon with an expected branching ratio of 10% in the presence of a 25-mT magnetic field [16]. The atoms in the 2^{3}S sublevel retain, with a good approximation, the original velocity distribution, since both recoil velocities for the absorption of a 205-nm photon ($\approx 1.8 \times 10^3$ ms^{-1}) and the emission of a 1312-nm photon ($\approx 2.8 \times 10^2$ ms^{-1}) are negligible. The UV pulse was delayed, with respect to the e^+ implantation time, from 20 ns (to let the electric field reach 0 V cm^{-1}) up to 65 ns by using an SRS DG645 digital delay generator.

The time distribution of γ rays emitted by e^+ and Ps annihilations, i.e., the so-called single-shot positron annihilation lifetime spectroscopy (SSPALS) spectrum, was acquired with the same procedure used in Refs. [16,33]. A 20 $\times$ 25 $\times$ 25-mm PbWO$_4$ scintillator, coupled to a Hamamatsu R11265-100 photomultiplier tube and digitized by a HD4096 Teledyne LeCroy oscilloscope, was placed 40 mm above the target (Fig. 1). In the presence of Ps formation, SSPALS spectra present a prompt peak, given by the fast 2γ annihilations of e^+ implanted in the target, and a tail that is dominated by the 3γ decay of Ps emitted into vacuum (Fig. 2). The changes in the Ps population induced by the interaction with laser light affect the area under the tail. This effect can be quantified by using the S parameter evaluated as

$$S = \frac{\mathcal{A}_{off} - \mathcal{A}_{on}}{\mathcal{A}_{off}}, \quad (1)$$

where $\mathcal{A}_{off}$ and $\mathcal{A}_{on}$ are the averages of the normalized areas $\mathcal{A}_{off}{}^i$ and $\mathcal{A}_{on}{}^i$ below the ith SSPALS shot, calculated in a given time window with lasers off and on, respectively [33].
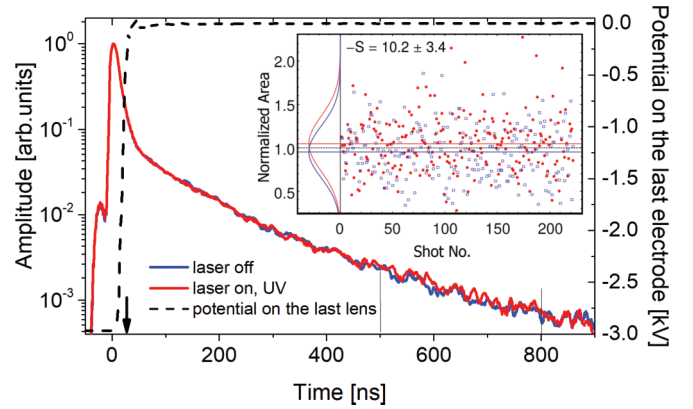

FIG. 2. Average of 200 SSPALS spectra of Ps in vacuum with UV laser off (blue) and on (red), normalized to the peak height. The potential on the focusing electrode is also shown (dashed line). The arrow marks the laser pulse instant (here 20 ns after the peak) and the vertical lines delimit the area used to conduct the detrending analysis of the S parameter shown in the inset (see text and Ref. [16]). Solid circles and empty squares are the detrended areas with and without laser (i.e., $\mathcal{A}_{on}{}^i$ and $\mathcal{A}_{off}{}^i$). The sideways Gaussian curves are the distributions of $\mathcal{A}_{on}{}^i$ (red) and $\mathcal{A}_{off}{}^i$ (blue).

The areas were normalized by using the detrending procedure described in Ref. [16], which mitigates the effect of eventual slow drifts in the positron beam intensity. The fraction of Ps excited to 3^{3}P with the UV pulse was evaluated by selectively photoionizing the excited atoms with an IR pulse ($\lambda_{IR} = 1064$ nm, energy of 50 mJ, and temporal FWHM of 4 ns [33]). The 1^{3}S-3^{3}P photoionization process results in a decrease of the Ps population decaying into 3γ at late times.

III. RESULTS AND DISCUSSION

Samples of 200 single SSPALS shots alternating UV + IR lasers on and off were collected with different laser delays to measure the 1^{3}S-3^{3}P excitation efficiency. A $S = (13.8 \pm 2.2)$% was observed in the selected 50–500 ns time window after the prompt peak for a laser delay of 20 ns, in agreement with the results of Refs. [16,33]. Repeating the measurement delaying the UV + IR laser pulses to 35 and 50 ns decreased the S signal by $\sim$30%, to $S = (8.8 \pm 2.6)$%, and by $\sim$60%, to $S = (6.8 \pm 2.9)$%, respectively, since an increasing fraction of Ps atoms had already left the target proximity before the laser pulse.

Sending the UV laser only, a fraction of the excited Ps is allowed to spontaneously decay from 3^{3}P to 2^{3}S. In the absence of an electric field, as in the present case, the lifetime of Ps in the 2^{3}S state is eight times longer than that in the 1^{3}S state (1140 ns vs 142 ns) [1,16]. Due to this longer lifetime, a larger fraction of atoms survives in-flight annihilation and reaches the experimental chamber walls, where it annihilates in 2γ with an electron of the medium producing a signal excess clearly identifiable in SSPALS spectra (Fig. 2).

A previously developed Monte Carlo (MC) code [16] was used to calculate the expected spatial and the temporal distributions of 1^{3}S and 2^{3}S annihilations in the geometry of our experimental chamber. This code calculates the atoms' flight trajectories and position and time annihilation distributions,

accounting for both in-flight self-annihilations and collisions with the walls, by integrating the equation of motion for the single particles and the optical rate equations of the internal level dynamics, while testing for collisions with the chamber walls. The final annihilation distributions are obtained upon averaging over the sample of atoms sorted on the initial velocity and position distributions. The free parameters are the $1\,^3\mathrm{S}$-$3\,^3\mathrm{P}$ excitation efficiency (obtained experimentally from the UV + IR data), the $3\,^3\mathrm{P}$-$1\,^1\mathrm{S}$ quenching efficiency (assumed to be 17% in our 25-mT magnetic field [16,33]), the $3\,^3\mathrm{P}$-$2\,^3\mathrm{S}$ branching efficiency (to be determined), and those specifying the initial position and velocity distributions. As no external electric field is present and the expected maximum motional Stark electric field is $\approx$25V cm^{-1} in our 25-mT magnetic field with a Ps velocity of the order of $\approx$10^5 ms^{-1} (corresponding to an optical decay rate of $2\,^3\mathrm{S}$ in an electric field of $\approx$100 kHz [16]), the optical decay of $2\,^3\mathrm{S}$ atoms was not included in the simulations. Ultimately the code produces a model estimate of the S parameter that can be directly compared with experimental data.

To give a pictorial representation of the expected annihilation positions of the $1\,^3\mathrm{S}$ and $2\,^3\mathrm{S}$ populations, a MC simulation has been conducted with 10^4 Ps atoms in each population (i.e., not reflecting the real $2\,^3\mathrm{S}$ and $1\,^3\mathrm{S}$ relative abundance to emphasize the rare annihilations of the $1\,^3\mathrm{S}$ fraction on the walls) and setting a uniform velocity of 10^5 ms^{-1} in modulus for all Ps atoms (Fig. 1). Isotropic emission of $1\,^3\mathrm{S}$ Ps from the converter and the Doppler selection from a $2\pi \times 120$ GHz excitation laser were assumed [31,33,36]. According to the MC simulations, around 60% of the produced $2\,^3\mathrm{S}$ Ps atoms reach the walls as opposed to only $\sim$1% of $1\,^3\mathrm{S}$ atoms with the same velocity. This causes the additional annihilations in the tail of the SSPALS spectra shown in Fig. 2, leading to negative values of the S parameter [Eq. (1)].

Experimentally, when the UV-laser delay is set to 20 ns, the excess of annihilations due to $2\,^3\mathrm{S}$ atoms reaching the chamber walls is observed between 500 and 800 ns from the peak maximum, giving $S = (-10.2 \pm 3.4)\%$ (Fig. 2, inset). The time when this excess appears can be controlled by varying the laser pulse delay.

Indeed, nanochanneled Si e^+-Ps converters emit Ps in a broad distribution of velocities [30,31]. Emission velocity is mostly dependent on the time needed to escape from the nanochannels into vacuum (or permanence time [28,29]): the highest values correspond to the shortest Ps permanence times (1 ns or less) and the lowest ones to the longest permanence times (up to 20 ns) [29,31]. As a matter of fact, the fraction that resides longer in the nanochannels loses more energy by collision with the walls. The UV laser pulse, thanks to its brief duration and its limited spatial dimension, excites only the fraction of the emitted Ps in front of the target at the time when the laser is shot. Ps atoms with different permanence times and consequently different velocities can be thus selected varying the laser timing.

Measurements as in Fig. 2 were repeated by retarding the UV-laser shot to 35, 50, and 65 ns. The $-S$ parameter was evaluated as a function of the time elapsed from the prompt peak in time windows of 300 ns with steps of 50 ns starting from 150 ns to highlight the excesses of Ps annihilations. The curves corresponding to the spectra acquired with the different
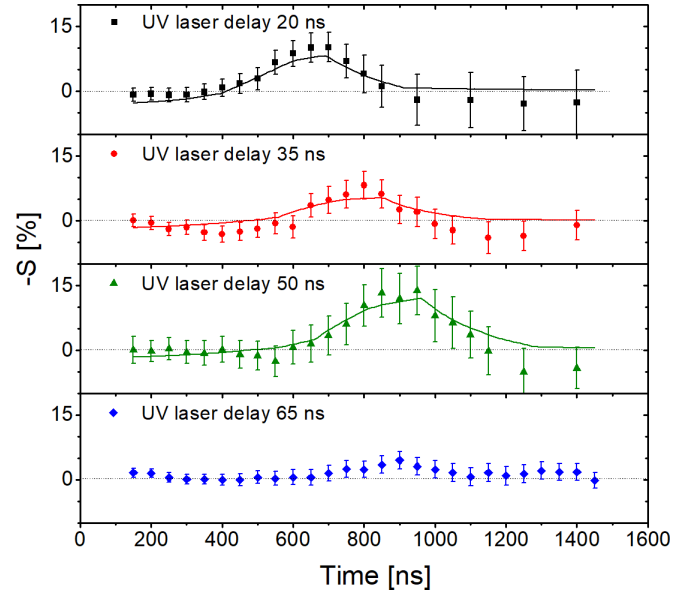

FIG. 3. $-S$ parameter as a function of the time elapsed from the prompt peak for different UV-laser delays (20, 35, 50, and 65 ns). The $-S$ parameter was calculated using time windows of 300 ns in steps of 50 ns. The continuous lines are the Monte Carlo best fits (see text) of the $-S$ parameter. The weak signal at 65 ns does not allow us to perform a reliable fit.

delay times are reported in Fig. 3 (each spectrum is obtained from a sample of 200 single shots).

The plot shows that the time of the annihilation excess, ascribable to $2\,^3\mathrm{S}$ (i.e., higher values of $-S$), is progressively time shifted by delaying the UV pulse. With a delay of 20 ns, the largest fraction of $2\,^3\mathrm{S}$ atoms reaches the walls of the chamber after 650–700 ns from the prompt (as also seen in Fig. 2). This time increases to 800 and 900 ns when the UV pulse is delayed to 35 and 50 ns, respectively. The excess of annihilations almost disappeared with 65 ns, indicating that the largest part of the Ps emitted by the converter has already left the laser spot. A rough estimation of the average velocity (for each delay setting) was promptly obtained considering the average distance between the converter and the front wall (6 cm, see Fig. 1): 6 cm/650ns $\simeq 1.0 \times 10^5$ ms^{-1}, 6 cm/800 ns $\simeq 8.0 \times 10^4$ ms^{-1}, and 6 cm/900 ns $\simeq 7.0 \times 10^4$ ms^{-1} for UV pulse delays of 20, 35, and 50 ns, respectively.

A more accurate estimation of the $2\,^3\mathrm{S}$ velocity distribution was obtained by fitting the experimental $-S$ versus time curves (Fig. 3) with the previously introduced MC model, assuming the initial $2\,^3\mathrm{S}$ Ps atoms velocities to be distributed as a one-dimensional Gaussian function in modulus and uniformly in angle. The initial position distribution was assumed to be pointlike as the e^+ spot radius of $\sim$1.5 mm is much smaller than other distances at play.

The superimposed solid lines in Fig. 3 were obtained from the MC calculations varying the $3\,^3\mathrm{P}$-$2\,^3\mathrm{S}$ efficiency and the average velocity to find the best agreement between data and predictions. The best-fit parameters and their statistical errors are summarized in Table I. The MC model fit agrees with the previous rough estimation of the average $2\,^3\mathrm{S}$ velocity for each

TABLE I. Comparison of the experimental $1\,^3$S-$3\,^3$P efficiency (from photoionization) and the best found parameters with the Monte Carlo model for different laser delays.

Laser delay	$1\,^3$S $\rightarrow$ $3\,^3$P efficiency	$3\,^3$P $\rightarrow$ $2\,^3$S efficiency	$2\,^3$S average velocity
20 ns	$(13.8 \pm 2.2)\%$	$(9.7 \pm 2.7)\%$	$(1.0 \pm 0.1) \times 10^5$ ms^{-1}
35 ns	$(8.8 \pm 2.6)\%$	$(8.7 \pm 5.0)\%$	$(0.8 \pm 0.1) \times 10^5$ ms^{-1}
50 ns	$(6.8 \pm 2.9)\%$	$(10.1 \pm 6.2)\%$	$(0.7 \pm 0.1) \times 10^5$ ms^{-1}

delay setting. Moreover, it constrains the standard deviation of each $2\,^3$S velocity distribution to $\Delta v < 1 \times 10^4$ ms^{-1} in all the three cases, pointing out that this source of $2\,^3$S is roughly monochromatic to $\Delta v/v \lesssim 14\%$ or better (the limit of our current sensitivity). A branching efficiency for the $3\,^3$P-$2\,^3$S transition of around 10%, in agreement with the expected theoretical value [16], was also found (Table I). Note that found values and error bars may be affected by unaccounted systematical uncertainties due to the approximated time, position and velocity distributions of emitted Ps, and laser excitation dynamics. However the results were verified not to be changing significantly (i.e., by more than 1.0×10^4 ms^{-1}) using other reasonable Ps emission models, for instance, uniform velocity and nonuniform angular emission with an angle cut at $60°$ or higher [31,36].

IV. CONCLUSIONS

In conclusion, we have demonstrated the possibility of producing $2\,^3$S Ps via $3\,^3$P excitation and spontaneous decay with a selected average velocity in the range 7–10 $\times 10^4$ ms^{-1} and with $\Delta v < 1 \times 10^4$ ms^{-1} ($< 14\%$ monochromaticity) in the absence of an electric field. With present positron-Ps converters [1,32] and bursts of 10^7 e^+ [37,38], 3–8 $\times 10^4$ Ps atoms every minute at the $2\,^3$S level can be obtained (according to the selected velocity range). Since the UV laser also acts as an angular selector due to its limited bandwidth, these $2\,^3$S Ps atoms expand in the space as depicted in Fig. 1. Using a proper angular selector, every minute an almost monochromatic pulsed beam of $\approx 1 \times 10^3$ $2\,^3$S atoms with an angular divergence of 50 mrad could be obtained. An enhancement of the beam intensity, while retaining the observed velocity selection, could be envisaged using stimulated emission, i.e., increasing the $3\,^3$P-$2\,^3$S transition rate and its branching effi-

ciency. Further reduction of the $2\,^3$S Ps atoms' velocity looks to also be feasible thanks to the observed thermal Ps emitted by similar e^+-Ps converters when held at cryogenic temperatures [30]. Selecting this thermal fraction should allow one to produce monochromatic $2\,^3$S with a velocity in the low range of 10^4 ms^{-1}. The development of long-lived $2\,^3$S Ps beams, with defined and tunable velocity, could open the possibility to perform interferometry measurements with Ps [8].

[1] D. B. Cassidy, Eur. Phys. J. D **72**, 53 (2018).

[2] C. Amole *et al.*, Nat. Commun. **4**, 1785 (2013).

[3] S. Aghion *et al.* (AEgIS Collaboration), Nat. Commun. **5**, 4538 (2014).

[4] P. Perez *et al.* (GBAR Collaboration), Hyperfine Interact. **233**, 21 (2015).

[5] A. Antognini *et al.*, Atoms **6**, 17 (2018).

[6] A. P. j. Mills and M. Leventhal, Nucl. Instrum. Methods Phys. Res., Sect. B **192**, 102 (2002).

[7] D. B. Cassidy and S. D. Hogan, Int. J. Mod. Phys.: Conf. Ser. **30**, 1460259 (2014).

[8] M. K. Oberthaler, Nucl. Instrum. Methods Phys. Res., Sect. B **192**, 129 (2002).

[9] D. B. Cassidy, T. H. Hisakado, H. W. K. Tom, and A. P. Mills, Phys. Rev. Lett. **108**, 043401 (2012).

[10] T. E. Wall, A. M. Alonso, B. S. Cooper, A. Deller, S. D. Hogan, and D. B. Cassidy, Phys. Rev. Lett. **114**, 173001 (2015).

[11] S. D. Hogan, EPJ Tech. Instrum. **3**, 2 (2016).

[12] A. C. L. Jones, J. Moxom, H. K. Rutbeck-Goldman, K. A. Osorno, G. G. Cecchini, M. Fuentes-Garcia, R. G. Greaves, D. J. Adams, H. W. K. Tom, A. P. Mills *et al.*, Phys. Rev. Lett. **119**, 053201 (2017).

[13] A. M. Alonso, B. S. Cooper, A. Deller, L. Gurung, S. D. Hogan, and D. B. Cassidy, Phys. Rev. A **95**, 053409 (2017).

[14] A. C. L. Jones, T. H. Hisakado, H. J. Goldman, H. W. K. Tom, and A. P. Mills, J. Phys. B **49**, 0064006 (2016).

[15] A. M. Alonso, S. D. Hogan, and D. B. Cassidy, Phys. Rev. A **95**, 033408 (2017).

[16] S. Aghion *et al.* (AEgIS Collaboration), Phys. Rev. A **98**, 013402 (2018).

[17] A. Miffre, M. Jacquey, M. Büchner, G. Trénec, and J. Vigué, Appl. Phys. B **84**, 617 (2006).

[18] K. F. Canter, A. P. Mills, Jr., and S. Berko, Phys. Rev. Lett. **34**, 177 (1975).

[19] T. D. Steiger and R. S. Conti, Phys. Rev. A **45**, 2744 (1992).

[20] D. J. Day, M. Charlton, and G. Laricchia, J. Phys. B **34**, 3617 (2001).

[21] G. Laricchia, M. Charlton, G. Clark, and T. C. Griffith, Phys. Lett. A **109**, 97 (1985).

[22] D. J. Murtagh, D. A. Cooke, and G. Laricchia, Phys. Rev. Lett. **102**, 133202 (2009).

[23] S. Chu and A. P. Mills, Phys. Rev. Lett. **48**, 1333 (1982).

[24] M. S. Fee, A. P. Mills, S. Chu, E. D. Shaw, K. Danzmann, R. J. Chichester, and D. M. Zuckerman, Phys. Rev. Lett. **70**, 1397 (1993).

[25] M. S. Fee, S. Chu, A. P. Mills, R. J. Chichester, D. M. Zuckerman, E. D. Shaw, and K. Danzmann, Phys. Rev. A **48**, 192 (1993).

[26] D. A. Cooke *et al.*, Hyperfine Interact. **233**, 67 (2015).

[27] S. Mariazzi, P. Bettotti, S. Larcheri, L. Toniutti, and R. S. Brusa, Phys. Rev. B **81**, 235418 (2010).

[28] D. B. Cassidy, T. H. Hisakado, V. E. Meligne, H. W. K. Tom, and A. P. Mills, Phys. Rev. A **82**, 052511 (2010).

[29] S. Mariazzi, L. Di Noto, G. Nebbia, and R. S. Brusa, J. Phys.: Conf. Ser. **618**, 012039 (2015).

[30] S. Mariazzi, P. Bettotti, and R. S. Brusa, Phys. Rev. Lett. **104**, 243401 (2010).

[31] F. Guatieri, Ph.D. thesis, University of Trento, 2018.

[32] S. Aghion *et al.* (AEgIS Collaboration), Nucl. Instrum. Methods Phys. Res., Sect. B **362**, 86 (2015).

[33] S. Aghion *et al.* (AEgIS Collaboration), Phys. Rev. A **94**, 012507 (2016).

[34] R. Caravita, Master's thesis, Università degli Studi di Milano, 2013.

[35] S. Cialdi, I. Boscolo, F. Castelli, F. Villa, G. Ferrari, and M. Giammarchi, Nucl. Instrum. Methods Phys. Res., Sect. B **269**, 1527 (2011).

[36] R. Caravita, Ph.D. thesis, Università degli Studi di Genova, 2017.

[37] J. R. Danielson, D. H. E. Dubin, R. G. Greaves, and C. M. Surko, Rev. Mod. Phys. **87**, 247 (2015).

[38] L. Liszkay, P. Comini *et al.*, J. Phys.: Conf. Ser. **443**, 012006 (2013).